Dalton Transactions

Cite this: *Dalton Trans.*, 2012, **41**, 54

www.rsc.org/dalton

PAPER

Cu^{II}-azide polymers with various molar equivalents of blocking diamine ligands: synthesis, structures, magnetic properties with DFT studies†

Sandip Mukherjee, Yogesh P. Patil and Partha Sarathi Mukherjee*

Received 11th July 2011, Accepted 1st September 2011
DOI: 10.1039/c1dt11312g

Four new neutral copper-azido polymers $[Cu_4(N_3)_8(Me\text{-}hmpz)_2]_n$ (**1**), $[Cu_4(N_3)_8(men)_2]_n$ (**2**), $[Cu_5(N_3)_{10}(N,N\text{-}dmen)_2]_n$ (**3**) and $[Cu_5(N_3)_{10}(N,N'\text{-}dmen)_5]_n$ (**4**) [Me-hmpz = 1-methylhomopiperazine; men = *N*-methylethylenediamine; *N*,*N*-dmen = *N*,*N*-dimethylethylenediamine and *N*,*N*′-dmen = *N*,*N*′-dimethylethylenediamine] have been synthesized by using various molar equivalents of the chelating diamine ligands with $Cu(NO_3)_2{\cdot}3H_2O$ and an excess of NaN_3. Single-crystal X-ray structures show that the basic asymmetric units of **1** and **2** are very similar, but the overall 1D structures were found to be quite different. Complex **3** with a different composition was found to be 2D in nature, while the 1D complex **4** with 1 : 1 metal to diamine ratio presented several new structural features. Cryomagnetic susceptibility measurements over a wide range of temperature were corroborated with density functional theory calculations (B3LYP functional) performed on the complexes **1–3** to provide a qualitative theoretical interpretation of their overall magnetic behavior.

Introduction

The research on metal coordination polymers has gained great recognition as an important interface between synthetic chemistry and materials science, and it provides a solid foundation to help understand how molecules can be organized to achieve the desired functions.[1] Among these, the molecular magnetic materials have received a special attention in the last two decades because of their potential applications in molecular switches, high-density information storage, quantum computation and so on.[2] Connecting paramagnetic centers by short bridges, in combination with incorporating different organic coligands to adjust the bridging structure and dimensionality, is a general strategy to design such materials.[3]

The azido group is among the most extensively studied short bridges, for its versatility in building extended networks and the diversity of the compounds in magnetic behavior.[4–10] This three-atom bridging ligand can bind two to four metal atoms in a variety of ways, which is important for both the architecture and the magnetic property of the complexes. The end-on (EO) bridging mode generally results in predictable exchange coupling depending mainly on the bridging angle; while the end-to-end (EE) mode mediates antiferromagnetic coupling with few exceptions.[4–10] To use these potentials to the full effect a judicial choice of the coligands as well as the control of stoichiometry is absolutely imperative, especially because most of these compounds are formed serendipitously.[10]

The dimensionalities and/or the overall structural architectures of the Cu-azido systems with neutral chelating ligands are determined by the relative molar quantities of copper and the ligand.[10] Higher equivalents of the chelating ligand reduces the available sites on the metal for coordination by the bridging azido ligand and thus generally leads to lower dimensional structures. A minor change in the substitution on these ligands can also dramatically alter the structure and magnetic behavior of the metal-azido systems.[10] This impelled us to see the effect of systematic changes in the amount of the blocking ligands on the structural change of the Cu-azido systems. We have recently shown these effects with a number of substituted ethylenediamines and also with a few tridentate ligands.[10d,f,i,j] These novel complexes with interesting structural and magnetic features encouraged us to see the effect of various other diamine ligands on the overall structure of the neutral copper-azido systems with various molar ratios. Here we report the synthesis, structural characterization, and variable-temperature magnetic behavior of four new Cu-azido coordination polymers $[Cu_4(N_3)_8(Me\text{-}hmpz)_2]_n$ (**1**), $[Cu_4(N_3)_8(men)_2]_n$ (**2**), $[Cu_5(N_3)_{10}(N,N\text{-}dmen)_2]_n$ (**3**), and $[Cu_5(N_3)_{10}(N,N'\text{-}dmen)_5]_n$ (**4**) [Me-hmpz = 1-methylhomopiperazine; men = *N*-methylethylenediamine; *N*,*N*-dmen = *N*,*N*-dimethylethylenediamine and *N*,*N*′-dmen = *N*,*N*′-dimethylethylenediamine] along with the theoretical treatment of **1–3** through density functional theory (DFT) studies. Among these, **1** and **2** have almost identical asymmetric cores with overall 1D structure, but the linking patterns of the

Department of Inorganic and Physical Chemistry, Indian Institute of Science, Bangalore, 560012, India. E-mail: psm@ipc.iisc.ernet.in; Fax: 91-80-23601552; Tel: 91-80-22933352

† Electronic supplementary information (ESI) available: X-Ray crystallographic data in CIF format, PXRD patterns, Curie–Weiss fitting of the $1/\chi_M$ *vs.* *T* data of **1–4** and atomic spin densities of the models used for DFT study. CCDC reference numbers 842479–842482. For ESI and crystallographic data in CIF or other electronic format see DOI: 10.1039/c1dt11312g

bridging azido ligands are very much different. Interestingly, reaction with *N*,*N*-dmen with similar initial stoichiometry, resulted in **3**, with a different ratio of metal to diamine, and an entirely different and novel structure. Complex **4** belongs to the family of copper-azido complexes with 1 : 1 metal to diamine ratio, but unlike most of these complexes it has a very complicated 1D structure.

Experimental section

Materials

$Cu(NO_3)_2 \cdot 3H_2O$, NaN_3, 1-methylhomopiperazine; *N*-methylethylenediamine; *N*,*N*-dimethylethylenediamine and *N*,*N*′-dimethylethylenediamine were obtained from commercial sources and used as received without further purification.

Physical measurements

Elemental analyses of C, H and N were performed using a Perkin–Elmer 240 C elemental analyzer. IR spectra were recorded as KBr pellets using a Magna 750 FT-IR spectrophotometer. The powder XRD data were collected using a D8 Advance X-ray diffractometer to verify the phase purity of these complexes (Fig. S1, ESI†). The measurements of variable-temperature magnetic susceptibility were carried out on a Quantum Design MPMS-XL7 SQUID magnetometer. Susceptibility data were collected using an external magnetic field of 0.2 T for all the complexes in the temperature range of 1.8 to 300 K. The experimental susceptibility data were corrected for diamagnetism (Pascal's tables).[11]

CAUTION! *Although we did not experience any problems with the compounds reported in this work, azido complexes of metal ions in the presence of organic ligands are potentially explosive. Only a small amount of material should be prepared, and it should be handled with care.*

Synthesis of complexes 1–4

To a 10 mL methanolic solution of $Cu(NO_3)_2 \cdot 3H_2O$ (1.00 mmol, 242 mg) and the appropriate diamine (0.50 mmol of Me-hmpz for **1**, men for **2**, *N*,*N*-dmen for **3** and 1.00 mmol of *N*,*N*′-dmen for **4**) an aqueous solution of NaN_3 (10.00 mmol, 650 mg) dissolved in 2 mL of water was added slowly. The mixture was stirred for 5 min and filtered. Slow evaporation of the filtrate (12–24 h) resulted in rectangular shaped black (**1–3**) or dark green (**4**) crystals suitable for X-ray diffraction and further studies.

Complex **1**: Isolated yield: ~ 55%. Anal. Calc. for **1**, $C_{12}H_{28}N_{28}Cu_4$: C, 17.60; H, 3.45; N, 47.90. Found: C, 17.88; H, 3.51; N, 47.65%. IR (KBr, cm^{-1}): 2026, 2081 and 2090(vs) for the azido groups. Complex **2**: Isolated yield: ~ 65%. Anal. Calc. for **2**, $C_6H_{20}N_{28}Cu_4$: C, 9.76; H, 2.73; N, 53.10. Found: C, 9.88; H, 2.98; N, 53.38%. IR (KBr, cm^{-1}): 2025, 2084 and 2094(vs) for the azido groups. Complex **3**: Isolated yield: ~ 42%. Anal. calc. for **3**, $C_8H_{24}N_{34}Cu_5$: C, 10.51; H, 2.65; N, 52.10. Found: C, 10.72; H, 2.39; N, 52.42%. IR (KBr, cm^{-1}): 2024, 2070 and 2089 for the azido groups. Complex **4**: Isolated yield: ~78%. Anal. Calc. for **4**, $C_{20}H_{60}N_{40}Cu_5$: C, 20.38; H, 5.13; N, 47.53. Found: C, 20.45; H, 5.32; N, 47.84%. IR (KBr, cm^{-1}): 2031, 2065 and 2083 for the azido groups.

X-Ray crystallographic data collection and refinements

Single-crystal X-ray data for **1–4** were collected on a Bruker SMART APEX CCD diffractometer using the SMART/SAINT software.[12] Intensity data were collected using graphite-monochromatized Mo-Kα radiation (0.71073 Å) at 293 K. The structures were solved by direct methods using the SHELX-97[13] program incorporated into WinGX.[14] Empirical absorption corrections were applied with SADABS.[15] All non-hydrogen atoms were refined with anisotropic displacement coefficients. The hydrogen atoms bonded to carbon and nitrogen were included in geometric positions and given thermal parameters equivalent to 1.2 times those of the atom to which they were attached. Structures were drawn using ORTEP-3 for Windows.[16] Crystallographic data and refinement parameters are shown in Table 1, and important interatomic distances and angles are given in Tables 2 (for **1** and **2**) and 3 (for **3** and **4**).

Computational methodology

The following computational methodology was used to calculate the exchange coupling constants in the reported complexes (**1–3**).[17–20] The phenomenological Heisenberg Hamiltonian $H = -\sum_{(i>j)} J_{ij} S_i S_j$ (where S_i and S_j are the spin operators of the paramagnetic metal centers *i* and *j*; and the J_{ij} parameters are the exchange-coupling constants for the different pair-wise interactions between the paramagnetic metal centers of the molecule) can be used to describe the exchange coupling between each pair of transition-metal ions present in the polynuclear complex to construct the full Hamiltonian matrix for the entire system.

To calculate the exchange coupling constants for any polynuclear complex with *n* different exchange constants, at least the energy of $n + 1$ spin configurations must be calculated. For example, in the case of the studied tetranuclear complexes, the exchange coupling values J_1 and J_2 were obtained by taking into account the energy of three different spin distributions: quintet with $S = 2$, triplet with $S = 1$ and singlet with $S = 0$.

The hybrid B3LYP functional[21] has been used in all calculations as implemented in *Gaussian 03* package.[22–25] The pseudo-potential LanL2DZ and triple-ζ quality basis set (TZVP) proposed by Ahlrichs and co-workers have been used for all atoms.[26] The calculations were performed on the complexes built from the experimental geometries.

Results and discussion

Synthesis

Complexes **1–3** were obtained from the reactions of $Cu(NO_3)_2 \cdot 3H_2O$ and 0.5 molar equivalents of chelating diamine ligands with excess of NaN_3 in a MeOH–H_2O mixture. As we have shown earlier,[10] the excess of NaN_3 normally ensures the prevention of the immediate precipitation of the copper-azido complex, allowing the crystallization of multidimensional compounds *via* self-assembly of the smaller units. It is interesting to note the differences in structures of these materials even with the same ratio of copper and diamines (**1** and **2**), and also the fact that under the same conditions and initial stoichiometry a differently substituted diamine (with an extra Me group) can afford crystals

Table 1 Crystallographic data and refinement parameters for **1–4**

	1	**2**	**3**	**4**
Empirical formula	$C_{12}H_{28}N_{28}Cu_4$	$C_6H_{20}N_{28}Cu_4$	$C_8H_{24}N_{34}Cu_5$	$C_{20}H_{60}N_{40}Cu_5$
M_r	818.78	738.66	914.31	1178.78
T/K	293 (2)	293(2)	293(2)	293(2)
Crystal system	Monoclinic	Triclinic	Triclinic	Monoclinic
Space group	$P2_1/n$	$P\bar{1}$	$P\bar{1}$	$C2/c$
a/Å	7.0267(15)	7.6280(3)	7.6737(3)	35.781(5)
b/Å	20.857(5)	8.2478(4)	9.4801(4)	9.4505(13)
c/Å	9.927(2)	9.9050(4)	11.3796(5)	15.367(2)
α/°	90.00	92.252(3)	113.678(2)	90.00
β/°	101.113(12)	91.946(3)	92.067(2)	109.974(3)
γ/°	90.00	98.562(3)	93.776(2)	90.00
V/Å^3	1427.6(5)	615.24(5)	754.73(5)	4883.7(12)
Z	4	2	1	4
D_c/g cm^{-3}	1.905	1.994	2.012	1.603
μ(Mo-Kα)/mm^{-1}	3.002	3.470	3.534	2.207
λ/Å	0.71073	0.71073	0.71073	0.71073
F(000)	824	368	455	2420
Collected reflns	52990	12310	11543	25594
Unique reflns	4391	3545	4513	4990
GOF (F^2)	1.041	0.972	1.041	1.009
R_1[a]	0.0546	0.0423	0.0279	0.0517
wR_2[b]	0.1266	0.1225	0.0677	0.0983

[a] $R_1 = \sum\|F_o\| - |F_c\|/\sum|F_o|$, [b] $wR_2 = [\sum\{w(F_o^2 - F_c^2)^2\}/\sum\{w(F_o^2)^2\}]^{1/2}$.

Table 2 Selected bond distances (Å) and angles (°) for **1** and **2**

1			
Cu(1)–N(1)	2.027(4)	Cu(1)–N(2)	1.990(4)
Cu(1)–N(3)	1.992(4)	Cu(1)–N(6)	1.990(4)
Cu(1)–N(14)$^{\#1}$	2.401(4)	Cu(2)–N(9)$^{\#2}$	2.470(4)
Cu(2)–N(9)	1.945(4)	Cu(2)–N(3)	2.042(3)
Cu(2)–N(6)	1.996(4)	Cu(2)–N(12)	1.949(4)
N(1)–Cu(1)–N(2)	78.61(15)	Cu(1)–N(3)–Cu(2)	101.03(15)
Cu(1)–N(6)–Cu(2)	102.72(16)	Cu(2)–N(9)–Cu(2)$^{\#2}$	93.76(15)
2			
Cu(1)–N(1)	2.017(3)	Cu(1)–N(2)	1.994(3)
Cu(1)–N(3)	1.990(3)	Cu(1)–N(6)	2.027(3)
Cu(1)–N(11)$^{\#3}$	2.419(3)	Cu(1)–N(12)$^{\#4}$	2.832(3)
Cu(2)–N(3)	1.991(3)	Cu(2)–N(6)	2.039(3)
Cu(2)–N(9)	1.979(3)	Cu(2)–N(12)	1.959(3)
Cu(2)–N(6)$^{\#4}$	2.436(3)		
N(1)–Cu(1)–N(2)	86.44(11)	Cu(1)–N(3)–Cu(2)	102.22(14)
Cu(2)–N(6)–Cu(1)	99.32(11)	Cu(2)$^{\#4}$–N(6)–Cu(1)	98.96(11)
Cu(1)–N(12)–Cu(2)	88.57(12)	Cu(2)$^{\#4}$–N(6)–Cu(2)	97.09(10)

Symmetry transformations used to generate equivalent atoms: $^{\#1}-x,-y,-z$. $^{\#2}-x+1,-y,-z$. $^{\#3}-x+1,-y,-z+1$. $^{\#4}-x,-y,-z+1$.

with different ratios of the metal and the diamine (compare **2** and **3**) and resulting in an entirely different structure. Complex **4** is also unique, in the sense that most of the other known 1 : 1 (copper: diamine) complexes with substituted ethylenediamine have been synthesized using 1 : 2 ratios of copper and azide;[27] the same attempt with *N*,*N*′-dmen was not successful. In fact using four equivalents of azide it is possible to isolate **4** with very low yields (~ 10–15%), and the yield increases with the increasing proportion of azide giving an optimum yield at the reported ratio. These facts emphasizes our earlier conclusion that it is more appropriate to call these 'syntheses' as 'crystallization techniques' instead.[10i] Intense and broad multiple infrared absorptions of azido stretching vibrations in the range from 2024 to 2094 cm^{-1}, are consistent with the presence of various bonding modes of the bridging azido ligands.

Structure description of $[Cu_4(N_3)_8(Me\text{-}hmpz)_2]_n$ (1) and $[Cu_4(N_3)_8(men)_2]_n$ (2)

These two 1D complexes have very similar dinuclear asymmetric unit structures (Fig. 1 and 2), but the tetranuclear basic units that they give rise to, are markedly different. For **1**, the basic tetranuclear structure can be viewed as a linear Cu^{II}_4 unit bridged by double end-on azido groups; while for **2** the Cu^{II}_4 units form incomplete dicubane clusters (Fig. 3).

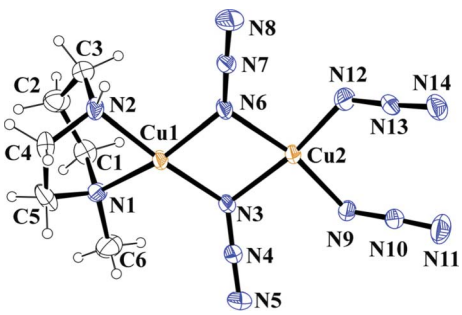

Fig. 1 ORTEP view of the asymmetric unit of **1**. Thermal ellipsoids are at 30% probability level.

For **1**, the asymmetric unit (Fig. 1) consists of two square-pyramidal Cu^{II} atoms, one chelating Me-hmpz ligand (linked to Cu1) and four azido groups. Cu1 has two nitrogen atoms from the diamine ligand (N1, N2) and two other $\mu_{1,1}$ nitrogen atoms (bridging to Cu2) of two azido ligand (N3, N6) in its basal plane with the bonds in the range 1.990(4) to 2.027(4) Å. The apical nitrogen atom is provided by one $\mu_{1,3}$ azido group [Cu1–N14$^{\#1}$, 2.401(4) Å]. Cu2 forms its basal bonds [1.945(4)–2.042(3) Å] with

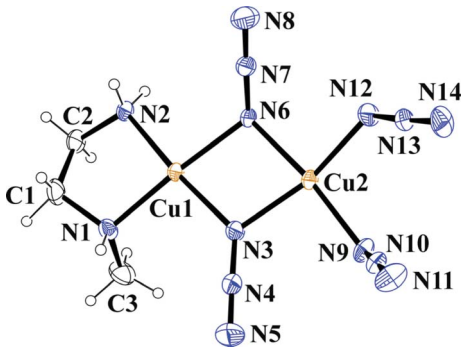

Fig. 2 ORTEP view of the asymmetric unit of **2**. Thermal ellipsoids are at 30% probability level.

two $\mu_{1,1}$ nitrogen atoms [N3, N6] that link to Cu1, another $\mu_{1,1}$ nitrogen atom that joins it with an adjacent Cu2 atom [N9] and one nitrogen atom from a $\mu_{1,3}$ azido group that links to the Cu1 atom of an adjacent Cu_4 unit [N12] and the apical nitrogen is provided by a $\mu_{1,1}$ nitrogen of an azido group that joins it to an adjacent Cu2 atom within the tetranuclear unit [Cu2–N9$^{\#2}$, 2.470(4) Å]. So, the two Cu^{II} atoms are joined together by symmetric double end-on (as all the bridging bonds are short, *i.e.*, <2.1 Å) azido bridges [Cu1–Cu2, 3.114(1) Å, Cu1–N3–Cu2, 101.03(15)°, Cu1–N6–Cu2, 102.72(16)°]. Two Cu2 atoms of two of these adjacent units are linked by asymmetric double end-on azido (as each bridging nitrogen atom forms a short and a long bond with the two metal atoms) bridges [Cu2–Cu2, 3.243(1) Å, Cu2–N9–Cu2$^{\#2}$, 93.76(15)°] and form the tetranuclear unit that repeats itself in one dimension. The adjacent Cu_4 units are joined by two end-to-end azido bridges (joining Cu1 and Cu2 atoms in adjacent Cu_4 units) and the chain runs along the crystallographic *a* axis (Fig. 3).

For **2**, Cu1 has a distorted octahedral geometry with two nitrogen atoms from the chelating ligand and two nitrogen atoms of two end-on azido ligands ($\mu_{1,1}$-N3 and $\mu_{1,1,1}$-N6) in its equatorial plane with the bonds in the range from 1.990(3) to 2.027(3) Å. The longer axial site is taken up by a $\mu_{1,1}$ nitrogen atom that joins it to Cu2 by asymmetric azido bridge within the Cu_4 unit [Cu1–N12$^{\#4}$, 2.832(3) Å]; while the shorter axial site is taken up by a nitrogen atom from a end-to-end bound azido group that joins it to a Cu2 atom of an adjacent Cu_4 unit [Cu1–N11$^{\#3}$, 2.419(3) Å]. Cu2 has a square-pyramidal geometry, with the basal sites [1.959(3)–2.039(3) Å] occupied by two $\mu_{1,1}$ nitrogen atoms [N3, N12], one $\mu_{1,1,1}$ nitrogen atom [N6] and another nitrogen atom [N9] from a end-to-end bound azido group that links it to the Cu1 atom of an adjacent unit. The apical position is taken up by a $\mu_{1,1,1}$ nitrogen atom within the unit [Cu2–N6$^{\#4}$, 2.436(3) Å]. Within the basic Cu^{II}_4 core, the Cu–N($\mu_{1,1}$/$\mu_{1,1,1}$)–Cu angles are spread within the range 88.57(12)–102.22(14)°. The adjacent Cu–Cu distances within the Cu_4 unit range from 3.099(1) to 3.403(1) Å, while that

Table 3 Selected bond distances (Å) and angles (°) for **3** and **4**

3			
Cu(1)–N(1)	2.047(2)	Cu(1)–N(2)	2.001(2)
Cu(1)–N(3)	2.015(2)	Cu(1)–N(6)	2.419(2)
Cu(1)–N(5)$^{\#5}$	1.999(2)	Cu(2)–N(9)$^{\#4}$	2.529(2)
Cu(2)–N(9)	1.970(2)	Cu(2)–N(12)	2.027(2)
Cu(2)–N(6)	1.953(2)	Cu(2)–N(15)	2.017(2)
Cu(3)–N(12)	1.990(2)	Cu(3)–N(15)	1.960(2)
N(1)–Cu(1)–N(2)	85.40(7)	Cu(1)–N(6)–Cu(2)	101.58(7)
Cu(2)–N(12)–Cu(3)	99.64(7)	Cu(2)–N(15)–Cu(3)	101.02(7)
4			
Cu(1)–N(1)	2.032(4)	Cu(1)–N(2)	2.029(4)
Cu(1)–N(3)	2.000(4)	Cu(1)–N(3)$^{\#6}$	2.614(4)
Cu(1)–N(6)	1.972(4)	Cu(1)–N(9)	2.597(4)
Cu(2)–N(11)	1.994(5)	Cu(2)–N(12)	2.022(4)
Cu(2)–N(13)	2.030(4)	Cu(2)–N(14)	1.993(4)
Cu(2)–N(17)	2.567(4)	Cu(2)–N(5)	2.775(5)
Cu(3)–N(17)	1.965(4)	Cu(3)–N(20)	2.015(4)
N(1)–Cu(1)–N(2)	84.46(14)	N(12)–Cu(2)–N(13)	84.37(16)
Cu(2)–N(17)–Cu(3)	102.18(13)	Cu(1)$^{\#6}$–N(3)–Cu(1)	97.90(14)

Symmetry transformations used to generate equivalent atoms: $^{\#5}$–*x*,–*y* + 1,–*z* + 1. $^{\#6}$–*x* + 3/2,–*y* + 3/2,–*z* + 1.

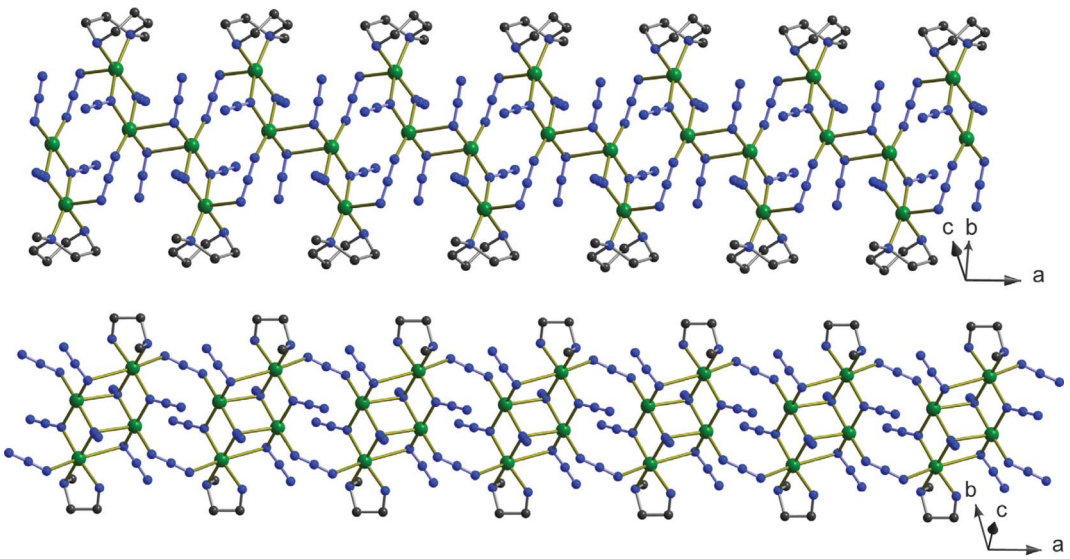

Fig. 3 Ball and stick view of the 1D arrangements of the Cu^{II}_4 units for **1** (top) and for **2** (bottom) illustrating their different connectivity. Color code: copper – green, nitrogen – blue, carbon – dark gray. Hydrogen atoms have been removed for clarity.

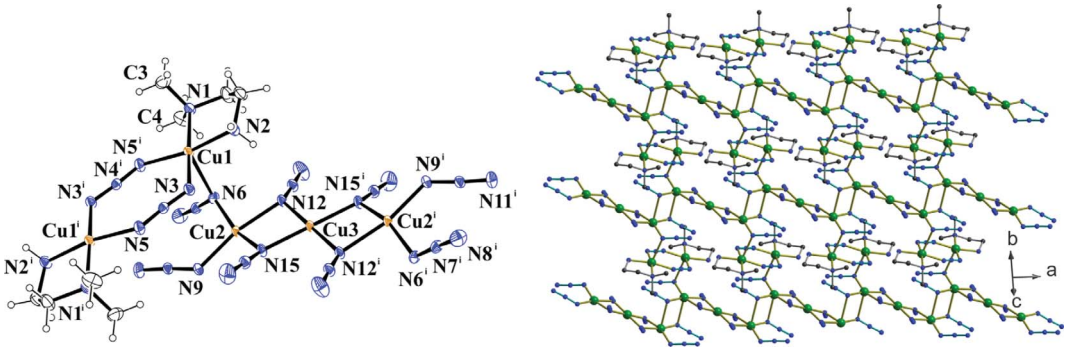

Fig. 4 ORTEP view of the basic unit (left, thermal ellipsoids are at 30% probability level) and the ball and stick representation of the overall 2D structure of **3** (right, hydrogen atoms have been removed for clarity; Color code: copper – green, nitrogen – blue, carbon – dark gray) (symmetry label, i: $1 - x, -y, 1 - z$).

for the neighboring units range from 4.727(1) to 5.108(1) Å. Thus the basic tetranuclear unit is formed by four doubly bridging and two triply bridging azido groups, while the neighboring units are held together by two end-to-end azido bridges to form an overall 1D structure that runs along the crystallographic *a* axis (Fig. 3).

From the structural point of view, it is very interesting to note the differences in the linking patterns of **1** and **2** as they have otherwise very similar dinuclear basic structures. To the best of our knowledge there is only one other structure known which resembles **2**,[10k] but **1** is unique. Incomplete double cubane units is fairly common in copper-azido chemistry,[10c,d,28] so probably the highly bulky Me-hmpz ligand does not allow the two dinuclear units to come close in space and results in a different overall structure for **1**.

Structure description of $[Cu_5(N_3)_{10}(N,N\text{-dmen})_2]_n$ (3)

Complex **3** crystallizes in the triclinic space group $P\bar{1}$ with three unique metal atoms and can be viewed as composed of Cu^{II}_5 basic units to form an overall 2D structure. The basic unit can be broken down to two centrosymmetric fragments, a dinuclear unit $[Cu_2(N,N\text{-dmen})_2(N_3)_2]^{2+}$ and a linear trinuclear unit $[Cu_3(N_3)_8]^{2-}$ (Fig. 4). The dinuclear unit is composed of two square-pyramidal Cu1 atoms chelated by the diamine ligand and linked by double end-to-end bound azido groups [Cu1–Cu1, 4.9992(4) Å; Cu1–N_{basal}, 1.999(2)–2.047(2) Å]; the apical nitrogen atom is provided by an end-on bridging azido group from an adjacent trinuclear unit [Cu1–N6, 2.419(2) Å]. The double symmetrical end-to-end azido bridges form an almost planar eight-member ring [torsion angle Cu1–N1–N3–Cu1 being 10.98°].[29] The linear trinuclear unit $[Cu_3(N_3)_8]^{2-}$ is composed of one square-planar Cu3 atom [Cu3–N12, 1.990(2) Å; Cu3–N15, 1.960(2) Å] at the center and two square-pyramidal Cu2 atoms [Cu2–N_{basal}, 1.953(2)–2.027(2) Å; Cu2–$N9^{\#4}_{apical}$, 2.529(2) Å] linked by double end-on (symmetric) azido bridges [Cu2–Cu3, 3.0691(3) Å; Cu2–N12–Cu3, 99.64(7)°; Cu2–N15–Cu3, 101.02(7)°]. These two subunits are joined together by a single asymmetric end-on azido bridge [Cu1–N6–Cu2, 101.58(7)°, Cu1–Cu2, 3.3998(5) Å] and the trinuclear units are also joined together head-to-tail by two end-on azido (asymmetric) bridges [Cu2–Cu2, 3.3472(4) Å, Cu2–N9–Cu2, 95.35(7)°] to give an overall two-dimensional structure (Fig. 4).

Structure description of $[Cu_5(N_3)_{10}(N,N'\text{-dmen})_5]_n$ (4). Single-crystal X-ray studies reveal that compound **4** consists of linear pentanuclear units, extended in one dimension. There are three metal atoms in the asymmetric unit, with one diamine ligand chelating each of them and six azido groups (Fig. 5). In the Cu^{II}_5 units the central Cu3 atom is linked to two adjacent Cu2 atoms through single end-on (asymmetric) azido bridges, and the Cu2 atoms are linked to the Cu1 atoms through double irregularly asymmetric end-to-end azido bridges (the two longer bridging bonds differ in length by ~0.3 Å). Cu1 atoms of two such neighbouring pentanuclear units are joined together by double end-on (asymmetric) azido bridges to form the chain that runs perpendicularly to the crystallographic *bc* plane (Fig. 6). Cu3 (which lies on a twofold axis) has a highly distorted square-planar geometry with two nitrogen atoms from a diamine and two nitrogen atoms from two end-on azido groups in its coordination sphere with bonds in the range from 1.965(4) to 2.015(4) Å. The planes extended by the two azido nitrogen atoms and the two diamine nitrogen atoms with the metal atom are at an angle of 24.78°. Cu2 has a distorted octahedral geometry with two nitrogen atoms from a diamine ligand, one nitrogen atom from an end-to-end bound (to Cu1) azido group and another nitrogen atom from a non-bridging azido group in its equatorial plane [Cu2–N_{eq}, 1.993(4)–2.030(4) Å]. The shorter axial site is taken up by a nitrogen atom from an end-on azido group [Cu2–N17, 2.567(4) Å] and the longer axial site is occupied by a nitrogen atom from a $\mu_{1,1,3}$ bridging azido group [Cu2–N5, 2.775(5) Å, shown

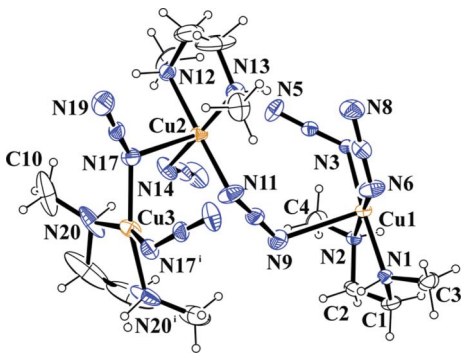

Fig. 5 ORTEP view of the asymmetric unit of **4**. Thermal ellipsoids are at 30% probability level (symmetry label, i: $1 - x, y, 1/2 - z$).

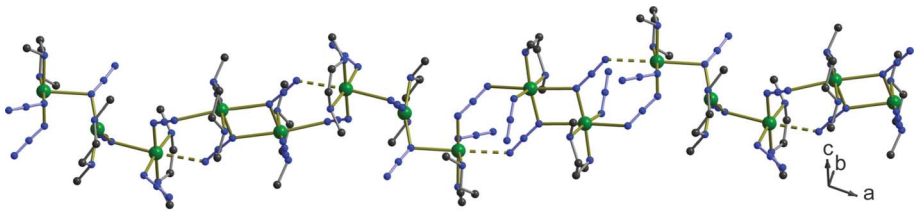

Fig. 6 Ball-and-stick view of the 1D arrangement of the Cu^{II}_5 units for **4**. Color code: copper – green, nitrogen – blue, carbon – dark gray. Hydrogen atoms have been removed for clarity.

as fragmented in Fig. 6]. Cu1 also has a distorted octahedral geometry, with two nitrogen atoms from a diamine ligand, one $\mu_{1,1}$ nitrogen (joining to a neighbouring Cu1 atom) atom from a $\mu_{1,1,3}$ azido group and another nitrogen atom from a non-bridging azido group in the equatorial sites [Cu1–N_{eq}, 1.972(4)–2.032(4) Å]. Unlike Cu2 the axial bonds for Cu1 are almost equal in length, with one nitrogen atom from an end-to-end bound (to Cu2) azido group [Cu1–N9, 2.597(4) Å] and another one $\mu_{1,1}$ nitrogen (joining to a neighbouring Cu1 atom) atom from a $\mu_{1,1,3}$ azido group [Cu1–N3$^{\#6}$, 2.614(4) Å]. The end-on bridging angles measure at 97.90(14) [Cu1–N3–Cu1] and 102.18(13)° [Cu2–N17–Cu3], and the neighbouring Cu–Cu distances (within the chain) range from 3.503(1) [Cu1–Cu1] to 5.273(1) Å [Cu1–Cu2].

The unique nature and sequence (two single asymmetric end-on, followed by double irregularly asymmetric end-to-end, followed by double asymmetric end-on and another double irregularly asymmetric end-to-end) of bridging azido groups to form a 1D copper chain is unprecedented in the literature. In fact the examples of single asymmetric end-on bridging and the double irregularly asymmetric azido bridging are also quite rare in the literature.[29d]

Magnetic behavior

Complex 1. The dc magnetic susceptibility measured on a polycrystalline sample of **1** under an applied field of 2000 G is shown in Fig. 7 as both χ_M *vs.* T and $\chi_M T$ *vs.* T plots (where χ_M is the molar magnetic susceptibility per Cu^{II}_4 unit). At room temperature (300 K) $\chi_M T$ value is 1.66 cm^3 K mol^{-1}, which is a little higher than expected for four uncoupled Cu^{II} ions ($\chi_M T$ = 0.375 cm^3 K mol^{-1} for an $S = 1/2$ ion with $g = 2.0$). The $\chi_M T$ value gradually increases upon lowering the temperature and shows a rapid jump below 50 K to reach a maximum value of 3.69 cm^3 K mol^{-1} at 6 K. Below this temperature the $\chi_M T$ value decreases sharply (saturation effect) to 2.31 cm^3 K mol^{-1} at 1.8 K. The $1/\chi_M$ *vs.* T plots (300–50 K) obey the Curie–Weiss law (Fig. S2, ESI†) with a positive Weiss constant of θ = 15.6(6) K, which along with the nature of the $\chi_M T$ *vs.* T plot indicates a dominant ferromagnetic interaction among the metal ions through azido bridges.

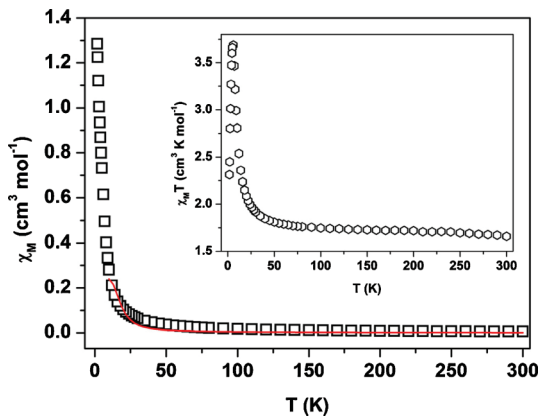

Fig. 7 Plots of χ_M *vs.* T and $\chi_M T$ *vs.* T (inset) for complex **1** in the temperature range of 1.8–300 K. The red solid line indicates the fitting using theoretical model (see text).

The magnetic exchange in the basic centrosymmetric core can be modeled as Cu(S_1)–J_1–Cu(S_2)–J_2–Cu(S_3)–J_1–Cu(S_4) (model A, Scheme 1) and as the two central Cu atoms are bridged by double asymmetric EO-azido bridges, while the peripheral Cu atoms are bridged by double symmetric EO-azido groups J_1 and J_2 are not expected to be identical.[10j] A reasonable fit can be obtained for interacting tetranuclear units applying the conventional Hamiltonian:

$$H = -J_1(S_1S_2 + S_3S_4) - J_2S_2S_3$$

introducing an inter-cluster zJ' term. Considering these three different exchange parameters, the analysis of the experimental susceptibility values has been performed using the following expression:

$$\chi_M = \chi_M'/\{1 - \chi_M'(2zJ'/Ng^2\beta^2)\}$$

$$\chi_M' = (Ng^2\beta^2/3kT)[A/B]$$

where $A = [30\exp(E_1/kT) + 6\exp(E_2/kT) + 6\exp(E_3/kT) + 6\exp(E_4/kT)]$ and $B = [5\exp(E_1/kT) + 3\exp(E_2/kT) + 3\exp(E_3/kT) + 3\exp(E_4/kT) + \exp(E_5/kT) + \exp(E_6/kT)]$;

$$E_1 = J_1/2 + J_2/4$$

$$E_2 = -J_1/2 + J_2/4$$

$$E_3 = -J_2/4 - (J_1^2 + J_2^2)^{1/2}/2$$

$$E_4 = -J_2/4 + (J_1^2 + J_2^2)^{1/2}/2$$

$$E_5 = -J_1/2 - J_2/4 - (4J_1^2 - 2J_1J_2 + J_2^2)^{1/2}/2$$

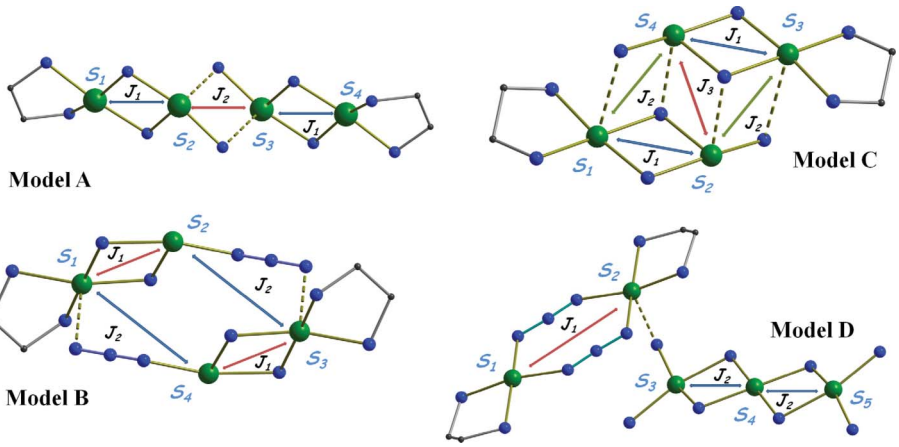

Scheme 1 Schematic diagrams representing the exchange interaction models used for complexes **1–3** (see text). The fragmented bonds are the longer axial or apical bonds.

$$E_6 = -J_1/2 - J_2/4 + (4J_1^2 - 2J_1J_2 + J_2^2)^{1/2}/2$$

The values giving the best fit (10–300 K) are $J_1 = +40.57(46)$ cm^{-1}, $J_2 = +28.47(26)$ cm^{-1}, $zJ' = -2.22(25)$ cm^{-1} and $g = 2.101(1)$ [$R = 2.07 \times 10^{-4}$].

The overall structure of this complex also allows us to use another fitting model B, as shown in Scheme 1, but the fitting was not found to be reasonable as compared to model A. J_1 is expected to have a moderate positive value as all the four end-on bridging bonds are short (average 2.01 Å) and the bridging angles (101.03 and 102.74°) are also lower than the cut-off angle of ~108°. However, for the central pair of the copper atoms although the bridging angle is quite lower (93.75°), the bridges are asymmetric with two short (1.95 Å) and two longer bonds (2.47 Å), so it's not surprising to find that $J_2 < J_1$.[29d] The end-to-end azido groups connecting the tetranuclear units can be considered to contribute towards the negative inter-cluster exchange.

Complex 2. Fig. 8 shows the temperature dependence of χ_M and $\chi_M T$ values for complex **2** (where χ_M is the molar magnetic susceptibility per Cu^{II}_4 unit). The room temperature (300 K) $\chi_M T$ value 1.75 cm^3 K mol^{-1}, is again slightly higher than expected for four uncoupled Cu^{II} ions and increases gradually up to 1.95 cm^3 K mol^{-1} upon lowering the temperature to 50 K. Below this temperature the $\chi_M T$ value decreases rapidly to 0.18 cm^3 K mol^{-1} at 1.8 K. The $1/\chi_M$ *vs.* T plots (300–50 K) obey the Curie–Weiss law (Fig. S2, ESI†) with a positive Weiss constant of $\theta = 5.7(4)$ K. The nature of the $\chi_M T$ *vs.* T plot and the small positive θ suggest that both ferromagnetic and antiferromagnetic exchanges are present among the four Cu^{II} ions through azido bridges.

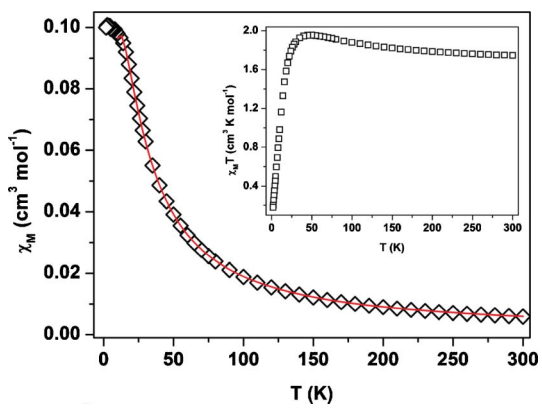

Fig. 8 Plots of χ_M *vs.* T and $\chi_M T$ *vs.* T (inset) for complex **2** in the temperature range of 1.8–300 K. The red solid line indicates the fitting using theoretical model (see text).

The structure of this complex suggests that both models B and C (Scheme 1) can be used to fit the magnetic data, but attempts to fit the data according to model C with or without inter-cluster exchange failed. But a reasonable fitting was obtained with model B for interacting tetranuclear units applying the Hamiltonian:[10k]

$$H = -J_1(S_1S_2 + S_3S_4) - J_2(S_1S_4 + S_2S_3)$$

introducing an inter-cluster zJ' term. Considering these three different exchange parameters, the analysis of the experimental susceptibility values has been performed using the following expression:

$$\chi_M = \chi_M'/\{1 - \chi_M'(2zJ'/Ng^2\beta^2)\}$$

$$\chi_M' = (Ng^2\beta^2/3kT)[A/B]$$

where $A = [30\exp(-E_1/kT) + 6\exp(-E_2/kT) + 6\exp(-E_3/kT) + 6\exp(-E_4/kT)]$ and $B = [5\exp(-E_1/kT) + 3\exp(-E_2/kT) + 3\exp(-E_3/kT) + 3\exp(-E_4/kT) + \exp(-E_5/kT) + \exp(-E_6/kT)]$;

$$E_1 = -J_1/2 - J_2/2$$

$$E_2 = -J_1/2 + J_2/2$$

$$E_3 = +J_1/2 - J_2/2$$

$$E_4 = +J_1/2 + J_2/2$$

$$E_5 = +J_1/2 + J_2/2 - (J_1^2 - J_1J_2 + J_2^2)^{1/2}$$

$$E_6 = +J_1/2 + J_2/2 + (J_1^2 - J_1J_2 + J_2^2)^{1/2}$$

The values giving the best fit (10–300 K) are $J_1 = +57.97(2.24)$ cm^{-1}, $J_2 = -14.03(7)$ cm^{-1}, $zJ' = +1.07(3)$ cm^{-1} and $g = 2.111(1)$ ($R = 1.43 \times 10^{-6}$).

The exchange parameter J_1 is attributed to the double symmetric end-on azido bridges with four short bridging bonds (average 2.01 Å), with the bridging angles (102.22 and 99.32°) well within the ferromagnetic domain, and the fitted value is also comparable to that of **1**. The weaker antiferromagnetic exchange (J_2) is mediated by the single end-to-end azido bridges, while the end-on azido bridges joining the tetranuclear magnetic clusters are responsible for the positive inter-cluster exchange.

Complex 3. The temperature dependence of magnetic susceptibility of **3** in the form of $\chi_M T$ and χ_M *vs.* T is displayed in Fig. 9. At room temperature, the value of $\chi_M T$ is 1.68 cm^3 K mol^{-1}, which is slightly lower than the expected value of 1.875 cm^3 K mol^{-1} ($g = 2$) for five uncoupled Cu^{II} ions. Upon cooling, the $\chi_M T$ value decreases slowly to reach a minimum value of 1.60 cm^3 K mol^{-1} at 190 K and then increases rather rapidly below to reach the value of 2.34 cm^3 K mol^{-1} at 6 K, and then again falls to 2.29 cm^3 K mol^{-1} at 1.8 K, indicating the presence of both ferromagnetic and antiferromagnetic couplings between the Cu^{II} ions. Accordingly, the $1/\chi_M$ *vs.* T plots (300–50 K) follow the Curie–Weiss law (Fig. S2, ESI†) with a positive Weiss constant of $\theta = 5.3(1.7)$ K.

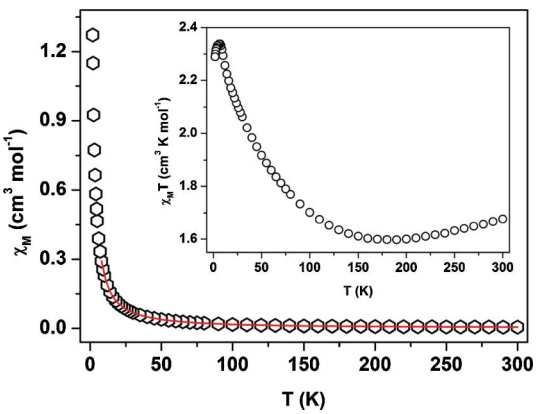

Fig. 9 Plots of χ_M *vs.* T and $\chi_M T$ *vs.* T (inset) for complex **3** in the temperature range of 1.8–300 K. The red solid line indicates the fitting using theoretical model (see text).

As illustrated in the structure description this complex can be viewed as composed of dinuclear and trinuclear units, and thus can be magnetically modeled as shown in Scheme 1 (model D) applying the Hamiltonian:

$$H = -J_1(S_1S_2) - J_2(S_3S_4 + S_4S_5)$$

Considering the weak interaction between trimer and dimer units, the susceptibility can be corrected by the mean-field, zJ' term.[30] Considering these three different exchange parameters, the analysis of the experimental susceptibility values has been performed using the following expression:

$$\chi_M = \chi_M'/\{1 - \chi_M'(2zJ'/Ng^2\beta^2)\}$$

$$\chi_M' = (2Ng^2\beta^2/kT)[3 + \exp(-J_1/kT)]^{-1} + (Ng^2\beta^2/4kT)[A/B]$$

where $A = [1 + \exp(J_2/kT) + 10\exp(3J_2/2kT)]$ and $B = [1 + \exp(J_2/kT) + 2\exp(3J_2/2kT)]$.

The values giving the best fit (8–300 K) are $J_1 = -494.99(18.80)$ cm^{-1}, $J_2 = +88.60(1.96)$ cm^{-1}, $zJ' = +0.187(5)$ cm^{-1} and $g = 2.122(2)$ [$R = 4.99 \times 10^{-8}$].

A very few examples are known in the literature[29] with double symmetric end-to-end azido bridges (with all short bonds, < 2.1 Å), and they are all found to mediate very strong antiferromagnetic exchange (500–1000 cm^{-1}), which is reflected in J_1. In the trinuclear units, the adjacent pairs of metal atoms are bridged by double symmetric azido groups with all short bonds (average 2.00 Å), with the bridging angles well below the cut-off mark (99.64 and 101.02°); so a moderately strong ferromagnetic exchange is expected. These units are joined together by single and double asymmetric end-on azido bridges, so the inter-cluster small positive exchange is also not surprising.

Complex 4. The magnetic susceptibility of **4** was measured in the 1.8–300 K temperature range at 2000 G, and they are shown as $\chi_M T$ and χ_M (where χ_M is the molar magnetic susceptibility per Cu$^{II}_5$ unit) *vs.* T plots (Fig. 10). The experimental $\chi_M T$ value of **4** at room temperature is 1.67 cm^3 K mol^{-1}, which is somewhat lower than the spin-only value (1.875 cm^3 K mol^{-1} for $g = 2$) expected for five magnetically isolated Cu^{II} ions. The $\chi_M T$ value gradually increases upon lowering the temperature to reach a maximum value of 2.03 cm^3 K mol^{-1} at 40 K. Below this temperature the $\chi_M T$ value decreases sharply to 0.49 cm^3 K mol^{-1} at 1.8 K. The $1/\chi_M$ *vs.* T plot above 50 K is linear following the Curie–Weiss law (Fig. S2, ESI†) with a positive $\theta = 16.53(1.81)$ K. The nature of these plots suggests the presence of exchange interactions of both sign between the metal ions through azido bridges.

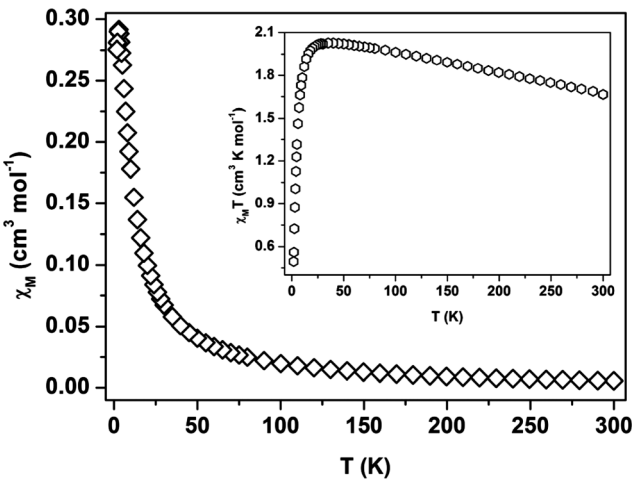

Fig. 10 Plots of χ_M *vs.* T and $\chi_M T$ *vs.* T (inset) for complex **4** in the temperature range of 1.8–300 K.

The chain consists of at least three very different exchange pairs as can be seen from the structure, so we were unable to construct a proper model to fit the magnetic data for **4**. Single end-on azido bridges joining three consecutive metal atoms are asymmetric with the bridging angle 102.18°, and thus a small ferromagnetic exchange is expected among these metal atoms. The next two copper atoms are joined by double asymmetric en-to-end azido bridges, which are expected to mediate antiferromagnetically. Finally the next two metal atoms are joined by double asymmetric

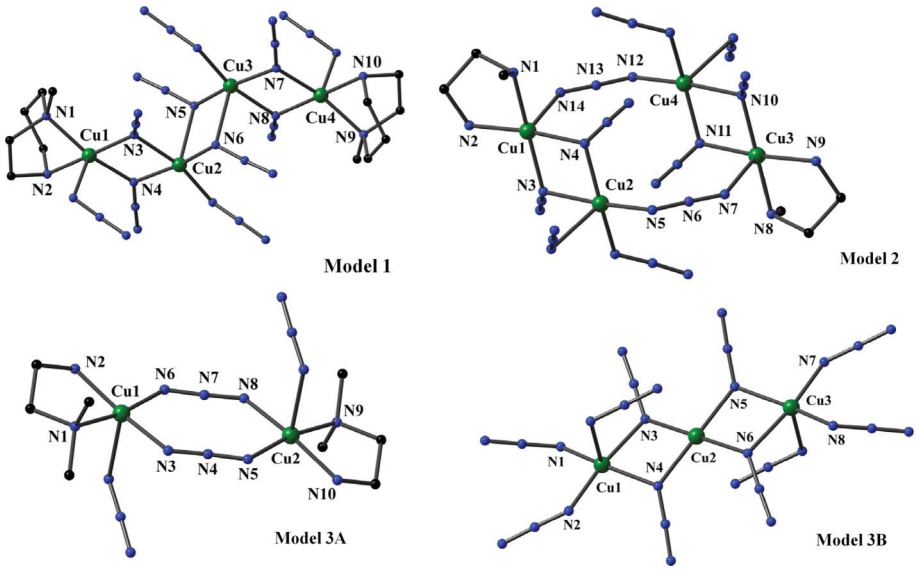

Scheme 2 Magnetic cores used for computational studies.

azido bridges with the bridging angle of 97.90°, so this pair is again expected to be ferromagnetically aligned. Thus the overall magnetic structure becomes very complicated and difficult to model.

Theoretical study

To better understand the magnetic exchange mechanism in the complexes **1**, **2** and **3** spin-unrestricted calculations were performed at the X-ray geometry (Scheme 2) using the *Gaussian 03* package at the B3LYP level employing the pseudo-potential LanL2DZ and the more complete TZVP basis sets for all atoms. The results of the theoretical studies (see the computational methodology section for details) in terms of the calculated exchange parameters are summarized in Table 4.

The calculations were performed with the models (for comparison) used for the magnetic fitting by filling up all the coordinating sites of the copper atoms (Scheme 2). To further check the validity of the calculations using larger models (tetranuclear) for **1** and **2**, the pair-wise exchange parameters were also calculated (Table 4).

The representations of the spin distributions corresponding to the ground spin states for **1** and **2** are plotted in Fig. 11 (for the complete representations and atomic spin density values of all the spin states see ESI†). As expected, the spin density distributions for the two peripheral pairs of metal atoms in the quintet ground states in **1** (Fig. 11) show the predominance of the delocalization mechanism through a σ type exchange pathway involving the $d_{x^2-y^2}$ magnetic orbitals of the Cu^{II} atoms and the sp^2 hybrid orbitals of the EO-azido nitrogen bridging atoms (with an average spin density of 0.113 e on the four nitrogen atoms), providing evidence for the moderately strong positive exchange observed experimentally. The smaller spin densities on the two nitrogen atoms (average 0.093 e) bridging the middle pair of metal atoms asymmetrically also points to a weaker interaction, supporting the experimental results. For **2**, the spin densities are quite largely delocalized over the nitrogen bridging atoms of the two end-to-end azido groups, as expected for singlet ground state.

Although some of the calculated values differ widely from the fitting values, in all the cases the sign and the relative magnitudes of the exchange parameters agree very nicely with the experimental results. It is difficult to say in general which basis set works better, but it is clear that both work only qualitatively. This may be due to the fact that the real complexes are not discrete entities as they have been modeled, but are quite complicated in their overall structures.

Table 4 Comparison of the experimental (from fitting) and DFT studies

			From DFT[a]	
Complex	J_i/cm^{-1}	Expt.	LanL2DZ	TZVP
1	J_1	+40.57	+102 (+155)	+79 (+114)
	J_2	+28.47	+55 (+77)	+53 (+69)
2	J_1	+57.97	+112 (+145)	+82 (+122)
	J_2	−14.03	−59 (−125)	−42 (−88)
3	J_1	−494.99	−868	−737
	J_2	+88.60	+81	+103

[a] The values in parentheses for **1** and **2** indicate the results obtained by calculating the exchange between the individual pairs of metal atoms.

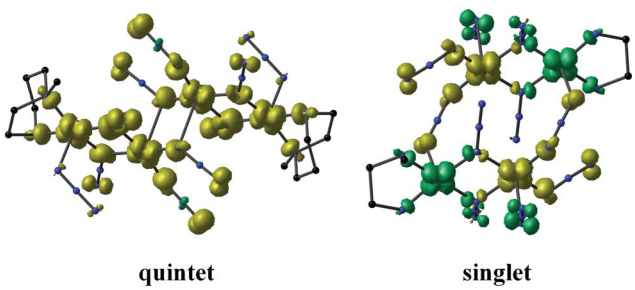

Fig. 11 Spin density maps calculated for the ground spin states of the model complexes **1** (left) and **2** (right) at B3LYP level (for LanL2DZ basis set). Positive and negative spin populations are represented as yellow and green surfaces. The isodensity surfaces correspond to a value of 0.007 e bohr^{-3}.

Concluding remarks

We have successfully implemented the strategy of using various metal to blocking ligand ratios to harness the versatility of the azido anion in binding metal ions together, to produce four new complexes. Among these complexes **1**, **3** and **4** have unprecedented structural topologies. The structural analysis shows that how a simple change in the structure of the blocking ligand can generate entirely different structures and magnetic properties, even though the basic structures seems to be almost identical (**1** and **2**). We have also shown that another blocking diamine does not produce similar complexes under the same reaction conditions, which leads us to questions as to whether certain compositions are forbidden? If not, what other methods can be used? Clearly, these questions deserve attention and more exploration.

Acknowledgements

S. M. and Y. P. P. gratefully acknowledge the Council of Scientific and Industrial Research, New Delhi, India for the award of a Research Fellowship. Authors also thank the Department of Science and Technology (DST) and CSIR, New Delhi for financial support.

References

1 (*a*) S. Kitagawa, R. Kitaura and S. I. Noro, *Angew. Chem., Int. Ed.*, 2004, **43**, 2334–2375; (*b*) R. E. Morris and P. S. Wheatley, *Angew. Chem., Int. Ed.*, 2008, **47**, 4966–4981; (*c*) Special Issue, *Acc. Chem. Res.*, 2005, **38**, 215–378; (*d*) Special Issue, *Chem. Soc. Rev.*, 2009, **38**, 1213; (*e*) L. J. Murray, M. Dincă and J. R. Long, *Chem. Soc. Rev.*, 2009, **38**, 1294–1314; (*f*) J. L. C. Rowsell and O. M. Yaghi, *Angew. Chem., Int. Ed.*, 2005, **44**, 4670–4679; (*g*) R. E. P. Winpenny, *Angew. Chem., Int. Ed.*, 2008, **47**, 7992; (*h*) C. F. Lee, D. A. Leigh, R. G. Pritcharg, D. Schults, S. J. Teat, G. A. Timco and R. E. P Winpenny, *Nature*, 2009, **458**, 314; (*i*) R. E. P. Winpenny, *J. Chem. Soc., Dalton Trans.*, 2002, 1; (*j*) V. Chandrasekhar, B. Murugesapandia, J. J. Vittal and R. Clérac, *Inorg. Chem.*, 2009, **48**, 1148; (*k*) S. Dalai, P. S. Mukherjee, T. Mallah, M. G. B. Drew and N. Ray Chaudhuri, *Inorg. Chem. Commun.*, 2002, **5**, 472.

2 (*a*) *Magnetism: Molecules to Materials*, ed. J. S. Miller and M. Drilon, Wiley-VCH, Weinheim, Germany, 2002–2005, vol. I–V; (*b*) O. Kahn, *Molecular Magnetism*, VCH, New York, 1993; (*c*) D. Gatteschi, O. Kahn, J. S. Miller and F. Palacio, *Magnetic Molecular Materials*, Kluwer Academic, Dordrecht, The Netherlands, 1991; (*d*) Special issue on Magnetism - Molecular, Supramolecular Perspectives, *Coord. Chem. Rev.*, 2005, **321**, 249; (*e*) *Molecular Magnetism: from Molecular Assemblies to Devices*, ed. E. Coronado, P. Delhaes, D. Gatteschi and J. S. Miller, NATO ASI Series 15, Kluwer, Dordrecht, The Netherlands, 1995.

3 (*a*) M. Ohba and H. Okawa, *Coord. Chem. Rev.*, 2000, **198**, 313; (*b*) S. R. Batten and K. S. Murray, *Coord. Chem. Rev.*, 2003, **246**, 103; (*c*) R. Lescouëzec, L. M. Toma, J. Vaissermann, M. Verdaguer, F. S. Delgado, C. Ruiz-Pérez, F. Lloret and M. Julve, *Coord. Chem. Rev.*, 2005, **249**, 2691; (*d*) J. Ribas, A. Escuer, M. Monfort, R. Vicente, R. Cortés, L. Lezama and T. Rojo, *Coord. Chem. Rev.*, 1999, **193–195**, 1027; (*e*) X.-Y. Wang, Z.-M. Wang and S. Gao, *Chem. Commun.*, 2008, 281; (*f*) A. Escuer and G. Aromí, *Eur. J. Inorg. Chem.*, 2006, 4721; (*g*) Y.-F. Zeng, X. Hu, F.-C. Liu and X.-H. Bu, *Chem. Soc. Rev.*, 2009, **38**, 469.

4 (*a*) G. S. Papaefstathiou, S. P. Perlepes, A. Escuer, R. Vicente, M. Font-Bardia and X. Solans, *Angew. Chem., Int. Ed.*, 2001, **40**, 884; (*b*) G. S. Papaefstathiou, S. P. Perlepes, A. Escuer, R. Vicente, M. Font-Bardia, X. Solans and S. P. Perlepes, *Chem. Commun.*, 2001, 2414; (*c*) A. K. Boudalis, B. Donnadieu, V. Nastopoulos, J. M. Clemente-Juan, A. Mari, Y. Sanakis, J.-P. Tuchagues and S. P. Perlepes, *Angew. Chem., Int. Ed.*, 2004, **43**, 2266; (*d*) P. K. Nanda, G. Aromí and D. Ray, *Inorg. Chem.*, 2006, **45**, 3143; (*e*) D. Mandal, V. Bertolasi, J. Ribas-Ariño and D. Ray, *Inorg. Chem.*, 2008, **47**, 3465; (*f*) P. Mukherjee, M. G. B. Drew, C. J. Gómez-García and A. Ghosh, *Inorg. Chem.*, 2009, **48**, 5848; (*g*) S. Chattopadhyay, M. G. B. Drew, C. Diaz and A. Ghosh, *Dalton Trans.*, 2007, 2492.

5 (*a*) S. Naiya, C. Biswas, M. G. B. Drew, C. J. Gómez-García, J. M. Clemente-Juan and A. Ghosh, *Inorg. Chem.*, 2010, **49**, 6616; (*b*) C. Biswas, M. G. B. Drew, E. Ruiz, M. Estrader, C. Diaz and A. Ghosh, *Dalton Trans.*, 2010, **39**, 7474.

6 (*a*) O. Kahn, *Chem. Phys. Lett.*, 1997, **265**, 165; (*b*) W. Ouellette, J. R. Galán-Mascaros, K. R. Dunbar and J. Jubieta, *Inorg. Chem.*, 2006, **45**, 1909; (*c*) M. Shatruk, A. Dragulescu-Andrasi, K. E. Chambers, S. A. Stoian, E. L. Bominaar, C. Achim and K. R. Dunbar, *J. Am. Chem. Soc.*, 2007, **129**, 6104; (*d*) T. K. Maji, P. S. Mukherjee, G. Mostafa, T. Mallah, J. Cano-Boquera and N. R. Chaudhuri, *Chem. Commun.*, 2001, 1012.

7 (*a*) D. J. Price, S. R. Batten, B. Moubaraki and K. S. Murray, *Chem. Commun.*, 2002, 762; (*b*) S. Konar, E. Zangrando, M. G. B. Drew, T. Mallah and N. R. Chaudhuri, *Inorg. Chem.*, 2003, **42**, 5966; (*c*) G. Leibeling, S. Demeshko, B. Bauer-Siebenlist, F. Meyer and H. Pritzkow, *Eur. J. Inorg. Chem.*, 2004, 2413; (*d*) S. Demeshko, G. Leibeling, S. Dechert and F. Meyer, *Dalton Trans.*, 2006, 3458.

8 (*a*) P. S. Mukherjee, T. K. Maji, G. Mostafa, T. Mallah and N. R. Chaudhuri, *Inorg. Chem.*, 2000, **39**, 5147; (*b*) J. Comarmond, P. Plumere, J. M. Lehn, Y. Agnus, R. Louis, R. Weiss, O. Kahn and I. Morgesten-Badarau, *J. Am. Chem. Soc.*, 1982, **104**, 6330; (*c*) J. Ribas, M. Monfort, B. K. Ghosh, X. Solans and M. Font-Bardía, *J. Chem. Soc., Chem. Commun.*, 1995, 2375; (*d*) J. Ribas, M. Monfort, B. K. Ghosh and X. Solans, *Angew. Chem., Int. Ed. Engl.*, 1994, **33**, 2087; (*e*) G. Viau, G. M. Lombardi, G. De Munno, M. Julve, F. Lloret, J. Faus, A. Caneschi and J. M. Clemente-Juan, *Chem. Commun.*, 1997, 1195; (*f*) A. Escuer, R. Vicente, J. Ribas, M. S. El Fallah, X. Solans and M. Font-Bardia, *Inorg. Chem.*, 1993, **32**, 3727; (*g*) E. Ruiz, J. Cano, S. Alvarez and P. Alemany, *J. Am. Chem. Soc.*, 1998, **120**, 11122; (*h*) Z. Shen, J.-L. Zuo, S. Gao, Y. Song, C.-M. Che, H.-K. Fun and X.-Z. You, *Angew. Chem., Int. Ed.*, 2000, **39**, 3633.

9 (*a*) A. Escuer, C. J. Harding, Y. Dussart, J. Nelson, V. McKee and R. Vicente, *J. Chem. Soc., Dalton Trans.*, 1999, 223; (*b*) A. Escuer, M. Font-Bardía, S. S. Massoud, F. A. Mautner, E. Penalba, X. Solans and R. Vicente, *New J. Chem.*, 2004, **28**, 681; (*c*) C. S. Hong and Y. Do, *Angew. Chem., Int. Ed.*, 1999, **38**, 193; (*d*) P. S. Mukherjee, S. Dalai, E. Zangrando, F. Lloret and N. R. Chaudhuri, *Chem. Commun.*, 2001, 1444; (*e*) S. Saha, S. Koner, J.-P. Tuchagues, A. K. Boudalis, K.-I. Okamoto, S. Banerjee and D. Mal, *Inorg. Chem.*, 2005, **44**, 6379; (*f*) L. K. Thompson, S. S Tandon and M. E. Manuel, *Inorg. Chem.*, 1995, **34**, 2356; (*g*) F. A. Mautner, S. Hanna, R. Cortés, L. Lezama, M. G. Barandika and T. Rojo, *Inorg. Chem.*, 1999, **38**, 4647.

10 (*a*) Z.-G. Gu, J.-L. Zuo and X.-Z. You, *Dalton Trans.*, 2007, 4067; (*b*) M. A. M. Abu-Youssef, A. Escuer, F. A. Mautner and L. öhrström, *Dalton Trans.*, 2008, 3553; (*c*) Z.-G. Gu, Y.-F. Xu, X.-J. Yin, X.-H. Zhou, J.-L. Zuo and X.-Z. You, *Dalton Trans.*, 2008, 5593; (*d*) K. C. Mondal and P. S. Mukherjee, *Inorg. Chem.*, 2008, **47**, 4215; (*e*) Q.-X. Jia, M.-L. Bonnet, E.-Q. Gao and V. Robert, *Eur. J. Inorg. Chem.*, 2009, 3008; (*f*) S. Mukherjee, B. Gole, R. Chakrabarty and P. S. Mukherjee, *Inorg. Chem.*, 2009, **48**, 11325; (*g*) C.-B. Tian, Z.-H. Li, J.-D. Lin, S.-T. Wu, S.-W. Du and P. Lin, *Eur. J. Inorg. Chem.*, 2010, 427; (*h*) O. Sengupta, B. Gole, S. Mukherjee and P. S. Mukherjee, *Dalton Trans.*, 2010, **39**, 7451; (*i*) S. Mukherjee and P. S. Mukherjee, *Inorg. Chem.*, 2010, **49**, 10658; (*j*) S. Mukherjee, B. Gole, Y. Song and P. S. Mukherjee, *Inorg. Chem.*, 2011, **50**, 3621; (*k*) S. Saha, D. Biswas, P. P. Chakrabarty, A. D. Jana, A. K. Boudalis, S. K. Seth and T. Kar, *Polyhedron*, 2010, **29**, 3342.

11 (*a*) R. L. Dutta and A. Syamal, *Elements of Magnetochemistry*, 2nd edn, East–West Press, Manhattan Beach, CA, 1993; (*b*) O. Kahn, *Molecular Magnetism*, VCH, New York, 1993.

12 *SMART*/*SAINT*, Bruker AXS, Inc., Madison, WI, 2004.

13 G. M. Sheldrick, *SHELX-97*, University of Göttingen, Göttingen, Germany, 1998.

14 L. J. Farrugia, *J. Appl. Crystallogr.*, 1999, **32**, 837; L. J. Farrugia, *WinGX*, version 1.65.04, Department of Chemistry, University of Glasgow, Glasgow, Scotland, 2003.

15 G. M. Sheldrick, *SADABS*, University of Göttingen, Göttingen, Germany, 1999.

16 ORTEP-3 for Windows, version 1.08: L. J. Farrugia, *J. Appl. Crystallogr.*, 1997, **30**, 565.

17 E. Ruiz, P. Alemany, S. Alvarez and J. Cano, *J. Am. Chem. Soc.*, 1997, **119**, 1297.

18 E. Ruiz, A. Rodríguez-Fortea, J. Cano, S. Alvarez and P. Alemany, *J. Comput. Chem.*, 2003, **24**, 982.
19 E. Ruiz, J. Cano, S. Alvarez and P. Alemany, *J. Comput. Chem.*, 1999, **20**, 1391.
20 E. Ruiz, *Struct. Bonding*, 2004, **113**, 71.
21 A. D. Becke, *J. Chem. Phys.*, 1993, **98**, 5648.
22 M. J. Frisch, G. W. Trucks, H. B. Schlegel, G. E. Scuseria, M. A. Robb, J. R. Cheeseman, J. A. Montgomery, Jr., T. Vreven, K. N. Kudin, J. C. Burant, J. M. Millam, S. S. Iyengar, J. Tomasi, V. Barone, B. Mennucci, M. Cossi, G. Scalmani, N. Rega, G. A. Petersson, H. Nakatsuji, M. Hada, M. Ehara, K. Toyota, R. Fukuda, J. Hasegawa, M. Ishida, T. Nakajima, Y. Honda, O. Kitao, H. Nakai, M. Klene, X. Li, J. E. Knox, H. P. Hratchian, J. B. Cross, V. Bakken, C. Adamo, J. Jaramillo, R. Gomperts, R. E. Stratmann, O. Yazyev, A. J. Austin, R. Cammi, C. Pomelli, J. Ochterski, P. Y. Ayala, K. Morokuma, G. A. Voth, P. Salvador, J. J. Dannenberg, V. G. Zakrzewski, S. Dapprich, A. D. Daniels, M. C. Strain, O. Farkas, D. K. Malick, A. D. Rabuck, K. Raghavachari, J. B. Foresman, J. V. Ortiz, Q. Cui, A. G. Baboul, S. Clifford, J. Cioslowski, B. B. Stefanov, G. Liu, A. Liashenko, P. Piskorz, I. Komaromi, R. L. Martin, D. J. Fox, T. Keith, M. A. Al-Laham, C. Y. Peng, A. Nanayakkara, M. Challacombe, P. M. W. Gill, B. G. Johnson, W. Chen, M. W. Wong, C. Gonzalez and J. A. Pople, *GAUSSIAN 03 (Revision B.04)*, Gaussian, Inc., Wallingford, CT, 2004.
23 A. D. Becke, *Phys. Rev. A: At., Mol., Opt. Phys.*, 1988, **38**, 3098.
24 C. Lee, W. Yang and R. G. Parr, *Phys. Rev. B*, 1988, **37**, 785.
25 E. Ruiz, S. Alvarez, J. Cano and V. Polo, *J. Chem. Phys.*, 2005, **123**, 164110.
26 A. Schäfer, C. Huber and R. J. Ahlrichs, *Chem. Phys.*, 1994, **100**, 5829.
27 (*a*) T. K. Maji, P. S. Mukherjee, S. Koner, G. Mostafa, J.-P. Tuchagues and N. R. Chaudhuri, *Inorg. Chim. Acta*, 2001, **314**, 111; (*b*) G. De Munno, M. G. Lombardi, M. Julve, F. Lloret and J. Faus, *Inorg. Chim. Acta*, 1998, **282**, 82; (*c*) L. Li, Z. Jiang, D. Liao, S. Yan, G. Wang and Q. Zhao, *Transition Met. Chem.*, 2000, **25**, 630; (*d*) A. Escuer, M. Font-Bardia, E. Penalba, X. Solans and R. Vicente, *Polyhedron*, 1998, **18**, 211; (*e*) S. Triki, C. J. Gómez-García, E. Ruiz and J. Sala-Pala, *Inorg. Chem.*, 2005, **44**, 5501.
28 K. C. Mondal, O. Sengupta and P. S. Mukherjee, *Inorg. Chem. Commun.*, 2009, **12**, 682.
29 (*a*) J. Comarmond, P. Plumeré, J. M. Lehn, I. Agnus, R. Louis, R. Weiss, O. Kahn and I. Morgenstern-Badarau, *J. Am. Chem. Soc.*, 1982, **104**, 6330; (*b*) Y. Agnus, R. Louis, J. P. Gisselbrecht and R. Weiss, *J. Am. Chem. Soc.*, 1984, **106**, 93; (*c*) P. Chaudhuri, K. Oder, K. Wieghart, B. Nuber and J. Weiss, *Inorg. Chem.*, 1986, **25**, 2818; (*d*) C. Adhikary and S. Koner, *Coord. Chem. Rev.*, 2010, **254**, 2933.
30 S.-H. Yan, X.-J. Zheng, L.-C. Li, D.-Q. Yuan and L.-P. Jin, *Dalton Trans.*, 2011, **40**, 1758.

